

ARTICLE

Reactions of a Diborylstannylene with CO₂ and N₂O: Diboration of Carbon Dioxide by a Main Group Bis(boryl) Complex

Received 00th January 20xx,
Accepted 00th January 20xx

DOI: 10.1039/x0xx00000x

Andrey V. Protchenko,^a M. Ángeles Fuentes,^a Jamie Hicks,^a Caitilín McManus,^a Rémi Tirfoin,^a and Simon Aldridge^{a,*}

The reactions of the boryl-substituted stannylene Sn{B(NDippCH)₂}₂ (**1**) with carbon dioxide have been investigated and shown to proceed via pathways involving insertion into the Sn–B bond(s). In the first instance this leads to formation of the (boryl)tin(II) borylcarboxylate complex Sn{B(NDippCH)₂}₂{O₂CB(NDippCH)₂} (**2**), which has been structurally characterized and shown to feature a κ^2 mode of coordination of the [(HCDippN)₂BCO₂][–] ligand at the metal centre. **2** undergoes B–O reductive elimination in hexane solution (in the absence of further CO₂) to give the boryl (borylcarboxylate) ester {(HCDippN)₂B}O₂C{B(NDippCH)₂} (**3**) i.e. the product of formal diboration of carbon dioxide. Alternatively, **2** can assimilate a second equivalent of CO₂ to give the homoleptic bis(borylcarboxylate) Sn{O₂CB(NDippCH)₂}₂ (**4**), which can be prepared via an alternative route from SnBr₂ and the potassium salt of [(HCDippN)₂BCO₂][–], and structurally characterized as its DMAP (*N,N*-dimethylaminopyridine) adduct. Structural and reactivity studies also point to the possibility for extrusion of CO from the [(HCDippN)₂BCO₂][–] fragment to generate the boryloxy system [(HCDippN)₂BO][–], a ligand which can be generated directly from **1** via reaction with N₂O. The initially formed unsymmetrical species Sn{B(NDippCH)₂}₂{OB(NDippCH)₂} has been shown to be amenable to crystallographic study in the solid state, but to undergo ligand redistribution in solution to generate a mixture of **1** and the bis(boryloxy) complex Sn{OB(NDippCH)₂}₂.

Introduction

Carbon dioxide sequestration/utilization is currently a hot topic, reflecting both socio-economic drivers and the fundamental challenges associated with its chemical transformation. In particular, reduction of CO₂ to more reactive feedstocks such as CO, HCOOH and CH₂O or to fuels such as CH₃OH and CH₄, as well as its conversion into complex organic or organometallic compounds are of significant interest.¹ A wide range of transition metal and main group element compounds has been implicated in such transformations in catalytic or stoichiometric fashion.² Within group 13–15 chemistry, Frustrated Lewis Pairs (FLPs) have emerged as a novel strategy for CO₂ capture/transformation,³ as have approaches involving insertion into E–H bonds to produce formate derivatives, which can be reduced further (even as far as methane) by using an appropriate hydride source (*e.g.*, for E = Al(III),⁴ Ga(III),⁵ Si(IV),⁶ Ge(II)).⁷ Another approach is to employ multiply-bonded compounds, which have been shown to give double-insertion products,⁸ either

reversibly (Ga=P)^{8a} or irreversibly (Al=Te).^{8b} Low-valent lighter p-block elements tend to reduce CO₂ to CO (*e.g.*, Si(II),⁹ Ge(I),¹⁰ Al(I))¹¹ or bind it into E–C(=O)–O–E' -containing moieties when more than one p-block element atom is involved (*e.g.*, B/B,¹² B/Al,¹³ Al/Al¹⁴).

On the other hand, examples of the activation of CO₂ by Sn(II) compounds are more scarce. Diaryl- and dialkylstannylenes are unreactive towards CO₂ (although examples of reactivity with CS₂ via Sn(II) to Sn(IV) oxidative pathways have been reported).¹⁵ The simple diamidostannylene Sn(NMe₂)₂ gives Sn–N insertion products with each of CO₂, COS and CS₂.^{16a} Similar insertion chemistry is observed with the heteroleptic system (NacNac)Sn(N^{*i*}Pr₂) [NacNac = CH(CMeNDipp)₂, Dipp = 2,6-C₆H₃^{*i*}Pr₂] leading to the formation of a β -diketiminatotin(II) carbamate.^{16b} Insertion of CO₂ into Sn–H bonds stabilised by bulky β -diketiminato,^{17a} amide^{7d} or aryl substituents^{17b} has been shown to generate the respective Sn(II) formates. Silylamido-substituted stannylenes are known to react in a more complex manner, due to the oxophilicity of silicon, resulting in silyl group migration from nitrogen to oxygen.¹⁸ Reversible coordination of carbon dioxide occurs with the *P,P*-chelated diphoshinamido stannylene Sn{N(P^{*i*}Pr₂)₂}₂, in which two molecules of CO₂ insert into the Sn–P bonds.¹⁹

Recently we reported on the reactivity of the boryl-substituted stannylene Sn{B(NDippCH)₂}₂ (**1**) towards E–H bonds, with oxidative addition taking place with nonpolar (E =

^a Inorganic Chemistry Laboratory, Department of Chemistry, University of Oxford, South Parks Road, Oxford, OX1 3QR, UK.
Email: simon.aldrige@chem.ox.ac.uk

Electronic Supplementary Information (ESI) available: [complete synthetic and characterizing data, representative NMR spectra, CIF files relating to the X-ray crystal structures]. See DOI: 10.1039/x0xx00000x

H), hydridic ($E = \text{B}, \text{Si}$) or acidic ($E = \text{N}, \text{O}$) bonds.²⁰ Oxidation of Sn(II) to Sn(IV) also occurs when **1** is treated with 2,3-dimethylbutadiene (via (1+4) cycloaddition) or with two equivalents of Ph_3CCl (via chlorine atom abstraction). In the current manuscript we report on the reactions of **1** with CO_2 and N_2O , which despite the potentially oxidizing nature of these two substrates, yield only Sn(II) products. The strongly oxophilic nature of the boryl substituents provides a thermodynamic driving force for insertion/rearrangement processes, leading in the case of carbon dioxide to the diboration of the CO_2 molecule under certain conditions.

Results and discussion

Reaction of diborylstannylene **1** with CO_2

In contrast to the redox reactivity of borylsilylene $\text{Si}\{\text{N}(\text{Dipp})\text{SiMe}_3\}\{\text{B}(\text{NDippCH})_2\}$ ^{9g} with carbon oxides, the reaction of stannylene **1** with CO_2 results in insertion rather than oxidation. The mono-insertion product **2** is formed at short reaction times (ca. 10 min, as monitored by ^1H and ^{11}B NMR), while storing the mixture under a CO_2 atmosphere for several days leads to the formation of the double insertion compound **4** as the major product (Scheme 1).

The unsymmetrical coordination environment in **2** is reflected in two sets of NMR signals for the boryl moieties, with the ^{11}B shifts being particularly diagnostic: $\delta_{\text{B}} = 58.1$ ppm for the Sn-bound B atom (cf. 96 ppm for the starting material **1**)²⁰ and upfield-shifted 19.8 ppm for the BCO_2 moiety. The latter is in the range of other compounds of the form $\{(\text{HCNDipp})_2\text{B}\}\text{C}(\text{X})=\text{O}$, e.g., $\{(\text{HCNDipp})_2\text{B}\}\text{C}(\text{OH})=\text{O}$, $\delta_{\text{B}} = 19.0$ ppm.²¹ Pale orange crystals of **2** were obtained from pentane at -30°C , and the resulting X-ray structure is shown in Figure 1. These crystallographic studies are consistent with a κ^2 mode of coordination for the borylcarboxylate ligand at tin, with the Sn–O bond lengths associated with the inserted CO_2 fragment being essentially identical (2.2313(16) and 2.2406(17) Å).

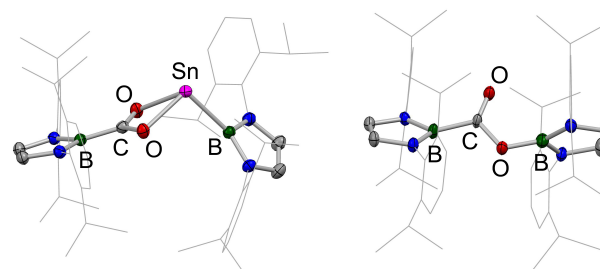
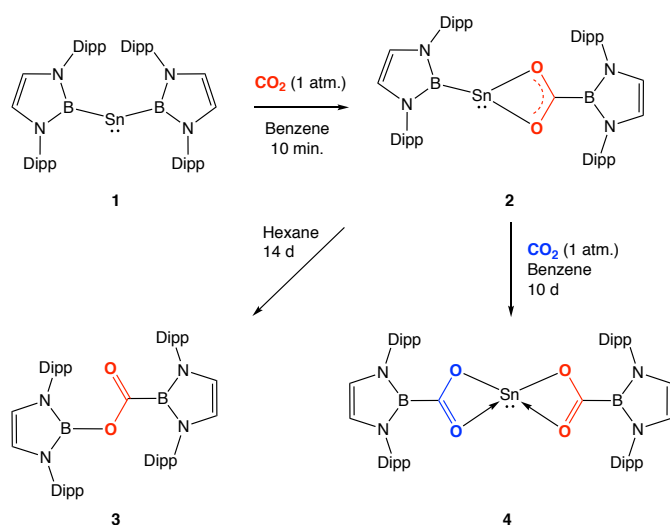


Figure 1. Molecular structures of (left) **2** and (right) **3** in the solid state as determined by X-ray crystallography. Hydrogen atoms and second (more disordered) molecule of **3** omitted, and Dipp groups shown in wireframe format for clarity; thermal ellipsoids set at the 40 % probability level. Key bond lengths (Å) and angles ($^\circ$) for **2**: Sn–B 2.297(2), Sn–O 2.2313(16), 2.2406(17), B–C 1.577(3), B–Sn–O 101.17(8), 97.90(8); for **3**: B–C 1.597(6), B–O 1.469(4), C–O 1.177(6), C–O(B) 1.375(6).

Compound **2** is highly soluble but thermally unstable in aliphatic hydrocarbons; prolonged storage of concentrated hexane solutions of **2** at room temperature result in a colour change from orange-yellow to very dark brown, and crystallisation of the colourless boryl borylcarboxylate ester **3** (Scheme 1). Crystalline **3** contains two independent molecules in the asymmetric unit, both having disorder in the central CO_2 moiety; the less disordered component and its structural metrics are shown in Figure 1. Compound **3** could also be synthesised independently from $\{(\text{HCNDipp})_2\text{B}\}\text{CO}_2\text{H}$ and $\{(\text{HCNDipp})_2\text{B}\}\text{Br}$, using NEt_3 as base.

3 can be regarded as being formed from **2** via reductive elimination of a B–O bond, with the overall transformation from **1**/ CO_2 amounting to the diboration of carbon dioxide. The net diboration of CO_2 has previously been reported by groups of Kinjo^{12a-d} and Harman.^{12e} The second product of the reductive elimination process, presumably a reduced tin species, crystallised as very thin microcrystals, which diffract too weakly for the X-ray crystallography. It should be noted that a related reductive elimination process leading to the generation of $\{(\text{HCNDipp})_2\text{B}\}\text{H}$ and $\{(\text{HCNDipp})_2\text{B}\}\text{NH}_2$ from $\text{H}(\text{H}_2\text{N})\text{Sn}\{\text{B}(\text{NDippCH})_2\}_2$ generates a mixture of tin metal and $\text{Sn}_{10}/\text{Sn}_{11}$ clusters as the metal-containing products.^{20b} Interestingly, and in contrast to its behaviour in hexane, **2** is stable in C_6D_6 under similar conditions. Such solvent dependence is surprising, but finds precedent in the chemistry of the indium boryl compound $\{(\text{MeCCH}_2)_2\}\{\text{In}\{\text{B}(\text{NDippCH})_2\}_2\}_2$ which decomposes in hexane solution to generate an $\text{In}_{19}\{\text{B}(\text{NDippCH})_2\}_6$ cluster.^{22a} Quantum chemical studies on somewhat related transformations including CO_2 activation by low valent silicon compounds have shown that aromatic solvents can significantly affect reaction rates through the involvement of C–H/ π interactions between the substrate and the solvent.^{22b}

Attempts to isolate the tin(II) bis(borylcarboxylate) (**4**) directly from the reaction of **1** with excess CO_2 gave only a viscous oil containing small amount of side-products, one of which gave rise to particularly high quality crystals from hexane solution, and which can thereby be identified as the



Scheme 1 Reaction of diborylstannylene **1** with CO_2 : insertion and reductive elimination chemistry.

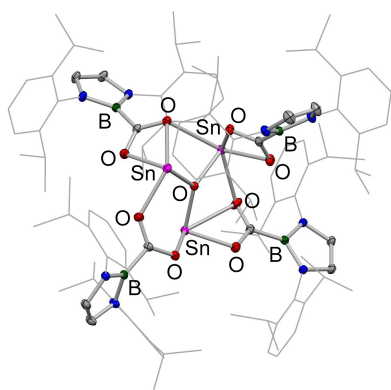


Figure 2. Molecular structure of **5** in the solid state as determined by X-ray crystallography. Hydrogen atoms omitted and Dipp groups shown in wireframe format for clarity; thermal ellipsoids set at the 40 % probability level. Key bond lengths (Å): Sn–O_{cent} 2.0777(15), 2.0878(14), 2.0890(14); C–B 1.580(3), 1.589(3), 1.582(3), 1.584(3).

trinuclear oxo-bridged tin(II) borylcarboxylate cluster $\text{Sn}_3(\mu_3\text{-O})\{\text{O}_2\text{CB}(\text{NDippCH}_2)_2\}_4$ (**5**; Figure 2). Although the origin of the bridging oxygen atom is not clear, a possible route involves CO elimination from the borylcarboxylate moiety of **4** to form a heteroleptic (borylcarboxylato)(boryloxy)tin species, which could generate a transient “SnO” moiety *in situ* via elimination of **3**. Formal combination of two molecules of **4** with “SnO” would produce the cluster **5**. It is of note that the elimination of CO from the borylcarboxylate moiety to give a boryloxy unit can be explicitly demonstrated in the presence of excess CO_2 for a related lithium derivative (see below).²³

Crystalline derivatives of tin(II) bis(borylcarboxylate) **4**

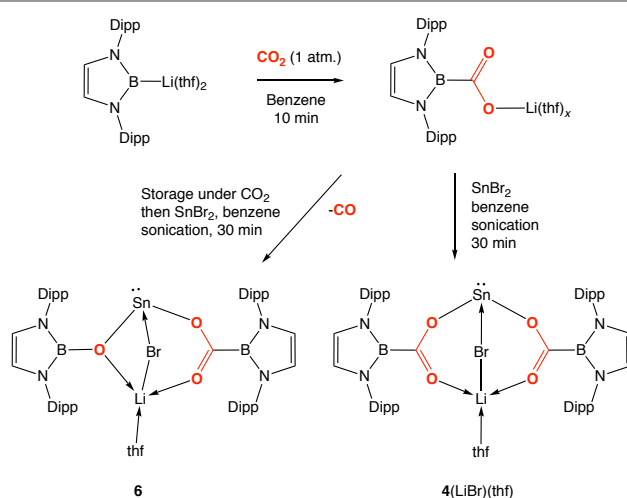
In order to unambiguously establish the nature of compound **4**, two alternative synthetic approaches were explored: (i) addition of the neutral donor 4-dimethylaminopyridine (DMAP) in an attempt to synthesize the corresponding Lewis base adduct (which might prove easier to crystallize); and (ii) an alternative synthesis of **4** itself utilizing salt metathesis from SnBr_2 and two equivalents of alkali metal borylcarboxylate. These strategies allowed a crystalline product to be isolated which could be characterised fully by spectroscopic, analytical and crystallographic methods.

We expected that salt metathesis method could provide an easier and cleaner route to **4**, avoiding the formation of **5** as a contaminant implicit in the reaction of **1** with CO_2 . Initially we planned to use the lithium borylcarboxylate for this metathesis chemistry (prepared *in situ* from Yamashita's boryllithium reagent and CO_2 ;²¹ Scheme 2). However this route proved to be unexpectedly complex. While the insertion of carbon dioxide into the Li–B bond occurs rapidly and cleanly by NMR, the solid product did not crystallise easily, and contained variable amounts of thf. In addition, when a freshly prepared solution of $(\text{thf})_2\text{LiO}_2\text{CB}\{\{\text{NDippCH}_2\}_2\}$ (showing one singlet for the backbone CH proton at $\delta_{\text{H}} = 6.07$ ppm) is stored overnight under a CO_2 atmosphere, several new signals appear (including a broad singlet for the backbone CH proton at $\delta_{\text{H}} = 6.01$ ppm and sharp signal at 5.95 ppm). Moreover, the ^{13}C NMR spect-

-rum measured at this point is even more complex, showing – among other things – a small sharp singlet at 184 ppm characteristic of carbon monoxide (see ESI). On the other hand, when independently synthesized $(\text{thf})_x\text{Li}\{\text{O}_2\text{CB}\{\{\text{NDippCH}_2\}_2\}\}$ is dissolved in C_6D_6 in the absence of excess CO_2 its ^1H NMR spectrum remains unchanged over a period of several days. This observation (and the isolation of tin complex **6** (see below)) suggests that excess CO_2 promotes the room-temperature decarbonylation of the borylcarboxylate anion (potentially by providing a less strained heterocyclic transition state than the three-membered ring proposed initially).²³ The involvement of an additional CO_2 molecule in decarbonylation by (CAAC)PhBAICp has recently been suggested by DFT calculations.¹³

Consistently, when a solution of $(\text{thf})_x\text{Li}\{\text{O}_2\text{CB}\{\{\text{NDippCH}_2\}_2\}\}$ (which had been stored under CO_2) was employed in a reaction with 0.5 equivalents of SnBr_2 , the heteroleptic compound $\text{Sn}\{\text{O}_2\text{CB}(\text{NDippCH}_2)_2\}_2\{\text{OB}(\text{NDippCH}_2)_2\}(\text{LiBr})(\text{thf})$ (**6**) was obtained after work up, which was characterised by multinuclear NMR spectroscopy and X-ray diffraction (Scheme 3). The crystal structure of this species (Figure 3) is consistent with the hypothesis that partial decarbonylation of the lithium borylcarboxylate had occurred, leading to formation of corresponding lithium boryloxide. By contrast, when a freshly prepared solution of the lithium borylcarboxylate was employed no such ligand degradation was observed. However, even under these conditions, the desired tin dicarboxylate was not obtained, but rather the corresponding adduct with $\text{LiBr}(\text{thf})$, $\text{Sn}\{\text{O}_2\text{CB}(\text{NDippCH}_2)_2\}_2(\text{LiBr})(\text{thf})$ (i.e. **4**)($\text{LiBr}(\text{thf})$; Scheme 2 and Figure 3).

With this in mind, and given the reduced propensity for potassium halide salts to be retained in this manner, we targeted a similar approach using the corresponding potassium borylcarboxylate (Scheme 3). This potassium derivative is most easily prepared from prepared from (known) $\{\text{HCNDipp}_2\text{B}\}\text{CO}_2\text{H}$ and KH, and could readily be obtained as single crystals, allowing characterization by X-ray crystallography as the distorted cubane-like tetramer $\{\text{KO}_2\text{CB}(\text{NDippCH}_2)_2\}_4$ (**7**) (see ESI).



Scheme 2 Reactions of lithium borylcarboxylate with SnBr_2 : synthesis of the ‘ate’ complexes **4**($\text{LiBr}(\text{thf})$) and **6**.

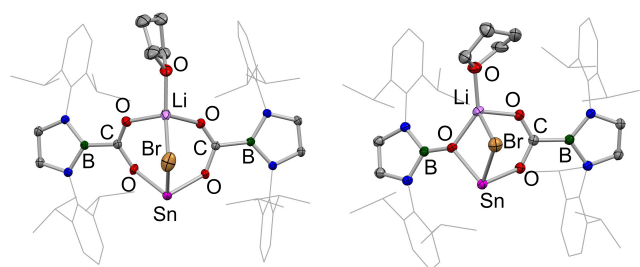
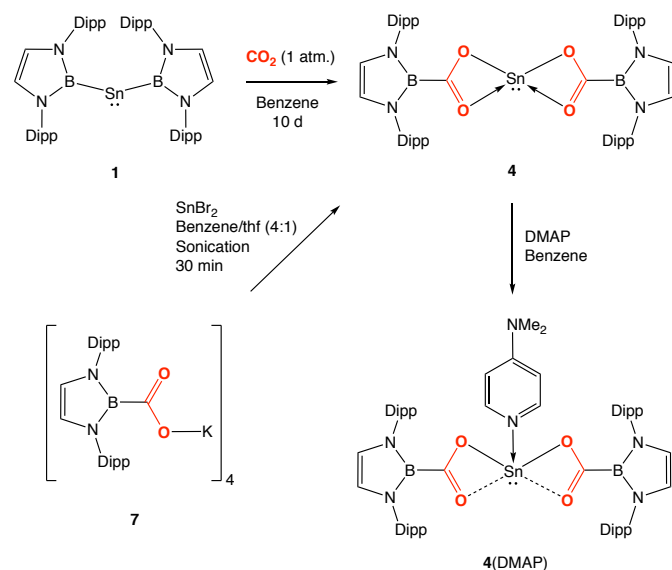


Figure 3. Molecular structures of (left) **4**(LiBr)(thf) and (right) **6** in the solid state as determined by X-ray crystallography. Hydrogen atoms omitted and Dipp groups shown in wireframe format for clarity; thermal ellipsoids set at the 40 % probability level. Key bond lengths (Å) for **4**(LiBr)(thf): Sn–O 2.0829(14), 2.0937(13); Sn–Br 2.6450(4); Li–Br 2.615(4); Li–O 1.878(4), 1.884(4), 1.936(10); for **7**: Sn–O 2.114(2), 2.122(2); Sn–Br 2.6428(5); Li–Br 2.748(7); Li–O 1.948(7), 1.916(7), 1.912(6).



Scheme 3 Generation and complexation of bis(borylcarboxylato)tin(II) compound **4**.

While **7** is fairly soluble in benzene, it did not react with SnBr_2 in this solvent; addition of thf (ca. 20 % by volume) and sonication, however, resulted in the formation of the desired tin dicarboxylate product which could be separated from KBr by removing the solvent *in vacuo* and extracting into hexane. Samples of **4** synthesized via this route display identical spectroscopic properties to those prepared from **1**/ CO_2 . Furthermore, addition of DMAP allows for the straightforward synthesis of the complex **4**(DMAP), which could readily be crystallised from warm hexane (Scheme 3). X-ray crystallography (Figure 4) reveals that the tin centre is best considered as three-coordinate, with only one oxygen atom of each of the potentially chelating carboxylate ligands engaging in a short contact ($d(\text{Sn}–\text{O}) = 2.132(2)$ and $2.143(2)$ Å) with the other interaction being somewhat longer ($d(\text{Sn}–\text{O}) = 2.697(2)$ and $2.714(2)$ Å). The O–Sn–O angle ($86.76(7)^\circ$) is narrower than the B–Sn–B angle of the starting stannylene **1** ($118.8(3)^\circ$) (and of related amine adducts of **1**), but similar to that of

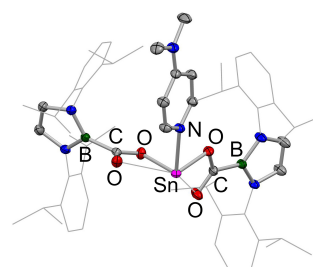
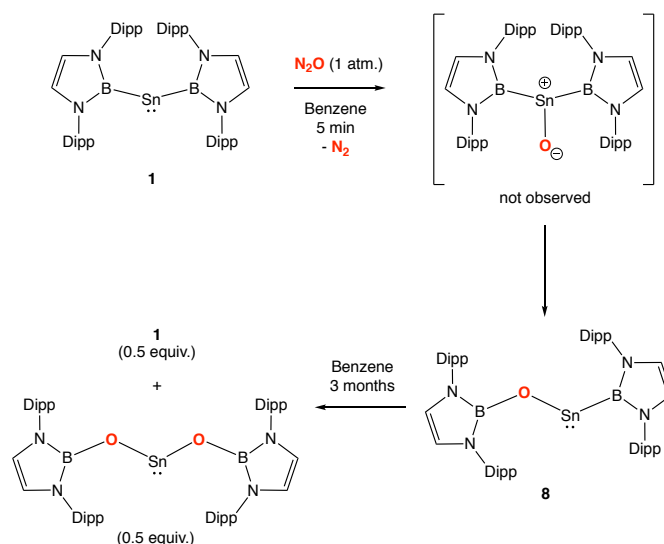


Figure 4. Molecular structure of **4**(DMAP) in the solid state as determined by X-ray crystallography. Hydrogen atoms omitted and Dipp groups shown in wireframe format for clarity; thermal ellipsoids set at the 40 % probability level. Key bond lengths (Å): Sn–O_{short} 2.132(2), 2.143(2); Sn–O_{long} 2.697(2), 2.714(2); Sn–N 2.291(2); O–Sn–O $86.76(7)^\circ$; N–Sn–O $89.03(7)$, $82.77(7)^\circ$.

$\text{Sn}\{\text{OB}(\text{NDippCH})_2\}_2$ ($93.3(1)^\circ$) – consistent with the tenets of Bent's rule and the more electronegative nature of oxygen over boron. The DMAP ligand is coordinated nearly perpendicular to the OSnO plane ($\angle(\text{N}–\text{Sn}–\text{O}) = 89.03(7)$ and $82.77(7)^\circ$). In this respect the overall coordination environment resembles those of the adducts of **1** with NH_3 and $t\text{BuNH}_2$.^{20b}

Reaction of diborylstannylene **1** with N_2O

The generation of the boryloxy ligand in **6** by formal decarbonylation chemistry led us to consider whether such a ligand system could be generated from **1** by the use of a more straightforward oxygen atom transfer reagent. As such, we turned our attention to the analogous chemistry with nitrous oxide. N_2O reacts readily with **1** under ambient conditions, as indicated by the colour change from yellow-green to dark purple. Monitoring the reaction mixture by ^1H and ^{11}B NMR spectroscopy shows that the initially formed unsymmetrical product **8** (Scheme 4) is unstable and in the presence of excess N_2O gives a complex mixture including the diazabutadiene



Scheme 4 Reaction of diborylstannylene **1** with N_2O : generation of mono- and bis(boryloxy) complexes via O-atom transfer and subsequent ligand redistribution chemistry.

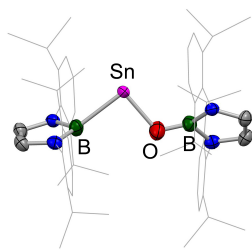


Figure 5. Molecular structure of **8** in the solid state as determined by X-ray crystallography. Hydrogen atoms and second disorder component omitted, and Dipp groups shown in wireframe format for clarity; thermal ellipsoids set at the 40% probability level. Due to significant disorder in the central BSnOB unit, no significant discussion of the geometric parameters of this unit is warranted.

derived from degradation of the boryl heterocycle. On the other hand, if excess N_2O is removed by the freeze/pump/thaw procedure, compound **8** could be isolated in single-crystalline form by recrystallization from benzene (Figure 5). Interestingly, however, redissolving crystalline samples of **8** in C_6D_6 reveals that it is unstable in solution towards ligand redistribution, yielding the bis(boryl) compound **1** and the (known) bis(boryloxy) derivative $\text{Sn}\{\text{OB}(\text{NDippCH})_2\}_2$, which were identified by ^1H NMR spectroscopy.²⁴ This process is relatively slow to reach equilibrium, with 10% conversion after 1 d, > 50% after 9 d and completion only after 3 months.

Conclusions

We have demonstrated that the reactions of both CO_2 and N_2O with diborylstannylene **1** result in Sn–B insertion products which retain the formal Sn(II) oxidation state, in contrast to the previously reported reactivity of silylenes towards the same oxide reagents. With CO_2 , sequential insertion into the Sn–B bonds produces hetero- (**2**) or homoleptic (**4**) tin(II) borylcarboxylate compounds. Compound **2** is thermally unstable in the absence of excess CO_2 , generating boryl borylcarboxylate ester **3** via formal B–O reductive elimination. This net transformation amounts to the stoichiometric diboration of carbon dioxide. With N_2O , insertion of an oxygen atom into one of the Sn–B bonds of **1** yields heteroleptic boryl(boryloxy)stannylene **8** (possibly via a transient stannone intermediate), which undergoes slow ligand redistribution in benzene solution to yield the corresponding symmetrical bis(boryl) and bis(boryloxy) stannylenes.

Experimental

General considerations

All manipulations were carried out using standard Schlenk line or dry-box techniques under an atmosphere of argon or dinitrogen. Hydrocarbon solvents were degassed by sparging with dinitrogen and dried by passing through a column of the appropriate drying agent and stored over Na or K mirror. Thf was refluxed over potassium-sodium alloy and distilled prior to use. NMR spectra were measured in C_6D_6 , which was dried over potassium, distilled under reduced pressure and stored

under dinitrogen in Teflon valve ampoules. NMR samples were prepared under dinitrogen in 5 mm Wilmad 507-PP tubes fitted with J. Young Teflon valves. ^1H and $^{13}\text{C}\{^1\text{H}\}$ NMR spectra were recorded on Bruker Avance III HD nanobay 400 MHz or Bruker Avance III 500 MHz spectrometer at ambient temperature unless stated otherwise and referenced internally to residual protio-solvent (^1H) or solvent (^{13}C) resonances and are reported relative to tetramethylsilane ($\delta = 0$ ppm). $^{11}\text{B}\{^1\text{H}\}$ NMR spectra were referenced to external $\text{Et}_2\text{O}\cdot\text{BF}_3$. Assignments were confirmed using two dimensional ^1H - ^1H and ^{13}C - ^1H NMR correlation experiments. Chemical shifts are quoted in δ (ppm) and coupling constants in Hz. Elemental analyses were carried out by London Metropolitan University. Starting materials **1** and $(\text{thf})_2\text{Li}\{\text{B}(\text{NDippCH})_2\}$ were synthesised according to published procedures.^{20,21} Carbon dioxide was stored in a Young's tap ampoule at 1 atm. pressure over P_2O_5 before use. $\{\text{HCNDipp}\}_2\text{B}\text{CO}_2\text{H}$ was made by a route similar to that described in ref 21, but we have found that it was necessary to use a strong acid (*p*-toluenesulfonic acid monohydrate, Aldrich) before flash chromatography in order to convert initially formed lithium carboxylate into free borylcarboxylic acid. Synthetic, spectroscopic and crystallographic data for $[\text{K}\{\text{O}_2\text{CB}(\text{NDippCH})_2\}]_4$ (**7**) are provided in the ESI.

Crystallography

Single-crystal X-ray diffraction data for all compounds were collected using an Oxford Diffraction Supernova dual-source diffractometer equipped with a 135 mm Atlas CCD area detector. Crystals were selected under Paratone-N oil, mounted on MiTeGen Micromount loops and quench-cooled using an Oxford Cryosystems open flow N_2 cooling device.^{25a} Data were collected at 150 K using mirror monochromated Cu $\text{K}\alpha$ radiation ($\lambda = 1.5418$ Å). Data collected were processed using the CrysAlisPro package,^{25b} including unit cell parameter refinement and inter-frame scaling (which was carried out using SCALE3 ABSPACK within CrysAlisPro). Equivalent reflections were merged and diffraction patterns processed with the CrysAlisPro suite.^{25b} Structures were solved ab initio from the integrated intensities using SHELXT^{25c} and refined on F^2 using SHELXL^{25d} with the graphical interface Olex2^{25e} or X-Seel.^{25f} Full details are given in the supplementary deposited CIF files (CCDC 2077133–2077140). These data can be obtained free of charge from the Cambridge Crystallographic Data Centre via http://www.ccdc.cam.ac.uk/data_request/cif.

Syntheses of novel compounds

Synthesis of $\text{Sn}\{\text{B}(\text{NDippCH})_2\}\{\text{O}_2\text{CB}(\text{NDippCH})_2\}$ (2**):** A solution of **1** (27 mg, 0.030 mmol) in C_6D_6 (0.5 mL) was degassed by the freeze/pump/thaw procedure, and the tube backfilled with CO_2 (to ca. 1 atm.) and gently shaken. The colour of the solution changed from yellow-green to light orange. A ^1H NMR spectrum measured at this point showed the formation of a single unsymmetrical product, but the starting stannylene **1** was not completely consumed. After shaking for 10 min the reaction was complete, with NMR measurements indicating near quantitative conversion. All

volatiles were removed *in vacuo*, and the resulting the oily residue dissolved in pentane (0.5 mL), transferred into crystallisation tube, concentrated to a smaller volume and stored at $-30\text{ }^{\circ}\text{C}$ overnight producing orange-yellow crystals of $\text{Sn}\{\text{B}(\text{NDippCH})_2\}\{\text{O}_2\text{CB}(\text{NDippCH})_2\}$ (**2**) suitable for X-ray diffraction. Compound **2** was highly soluble (and thermally unstable, *vide infra*) in aliphatic hydrocarbon solvents even at low temperature so that only few crystals could be isolated; however, the ^1H NMR spectrum of the crystals was nearly identical (apart from signals of the crystallisation solvent pentane and minor decomposition products) to the spectrum of *in situ* prepared sample. ^1H NMR (C_6D_6 , 298 K): δ_{H} 7.05–7.19 (12H, m, CH of Ar + $\text{C}_6\text{D}_5\text{H}$), 6.18 (2H, s, NCH), 6.01 (2H, s, NCH), 3.16 (4H, septet, $^3J = 6.9\text{ Hz}$, CHMe_2), 3.10 (4H, septet, $^3J = 6.9\text{ Hz}$, CHMe_2), 1.24 (12H, septet, $^3J = 6.9\text{ Hz}$, CHMe_2), 1.17 (12H, septet, $^3J = 6.9\text{ Hz}$, CHMe_2), 1.17 (12H, septet, $^3J = 6.9\text{ Hz}$, CHMe_2), 1.13 (12H, septet, $^3J = 6.9\text{ Hz}$, CHMe_2), 1.07 (12H, septet, $^3J = 6.9\text{ Hz}$, CHMe_2). ^{13}C -NMR (C_6D_6 , 298 K): δ_{C} 190.0 (br, BCO_2), 145.8 (*o*-C of Ar), 145.7 (*o*-C of Ar), 139.2 (*ipso*-C of Ar), 138.7 (*ipso*-C of Ar), 127.8 (*p*-CH of Ar, overlapping with $\text{C}_6\text{D}_5\text{H}$), 123.6 (*m*-CH of Ar), 123.4 (*m*-CH of Ar), 121.7 (NCH), 120.6 (NCH), 28.7 (CHMe_2), 28.7 (CHMe_2), 25.0 (CHMe_2), 24.9 (CHMe_2), 24.3 (CHMe_2), 24.1 (CHMe_2). $^{11}\text{B}\{^1\text{H}\}$ (C_6D_6 , 298 K): δ_{B} 58.1 (BSn), 19.8 (BCO_2).

Decomposition of 2 (isolation of 3 and 5): A sample of **2** prepared as above was dissolved in hexane (0.5 mL) and the tube sealed under vacuum. The concentrated solution failed to produce crystals at $-30\text{ }^{\circ}\text{C}$ for several days, so it was stored at room temperature. Initially, after 1 d, a small amount (less than 5%) of very well shaped rhombic colourless crystals was formed, which were identified by X-ray diffraction as $\text{Sn}_3\{\text{O}_2\text{CB}(\text{NDippCH})_2\}_4(\mu_3\text{-O})$ (**5**). The remaining solution was stored for two weeks, while slowly darkening to brown and almost black, then concentrated again producing large colourless blocks, which were washed with a small amount of cold hexane and dried *in vacuo* yielding $\{\text{HCNDipp}\}_2\text{B}\{\text{CO}_2\}\{\text{B}(\text{NDippCH})_2\}$ (**3**) (21 mg, 0.025 mmol, 67 %). From the mother liquor black (dark brown when crushed) crystals precipitated which were of insufficient quality/size for X-ray diffraction. Characterizing data for **3**: Anal. found (calcd. for $\text{C}_{53}\text{H}_{72}\text{B}_2\text{N}_4\text{O}_2$): C, 77.82 (77.75); H, 9.05 (8.86); N, 6.80 (6.84) %. ^1H NMR (C_6D_6 , 298 K): δ_{H} 7.14–7.20 (4H, m, *p*-CH of Ar + $\text{C}_6\text{D}_5\text{H}$), 7.02–7.05 (8H, m, *m*-CH of Ar), 5.89 (2H, s, NCH), 5.88 (2H, s, NCH), 3.15 (4H, septet, $^3J = 6.9\text{ Hz}$, CHMe_2), 2.94 (4H, septet, $^3J = 6.9\text{ Hz}$, CHMe_2), 1.24 (12H, septet, $^3J = 6.9\text{ Hz}$, CHMe_2), 1.13 (12H, septet, $^3J = 6.9\text{ Hz}$, CHMe_2), 1.10 (12H, septet, $^3J = 6.9\text{ Hz}$, CHMe_2), 0.97 (12H, septet, $^3J = 6.9\text{ Hz}$, CHMe_2), 0.95 (12H, septet, $^3J = 6.9\text{ Hz}$, CHMe_2). $^{13}\text{C}\{^1\text{H}\}$ NMR (C_6D_6 , 298 K): δ_{C} 175.5 (very broad, only observed in HMBC, BCO_2), 146.7 (*o*-C of Ar), 146.7 (*o*-C of Ar), 138.6 (*ipso*-C of Ar), 138.0 (*ipso*-C of Ar), 127.9 (*p*-CH of Ar), 127.6 (*p*-CH of Ar), 123.6 (*m*-CH of Ar), 123.4 (*m*-CH of Ar), 120.6 (NCH), 118.6 (NCH), 28.7 (CHMe_2), 28.5 (CHMe_2), 25.3 (CHMe_2), 24.7 (CHMe_2), 23.9 (CHMe_2), 23.8 (CHMe_2). $^{11}\text{B}\{^1\text{H}\}$ (C_6D_6 , 298 K): δ_{B} 21.4 (br), 19.5 (br).

Alternative synthesis of 3: A mixture of $\{\text{HCNDipp}\}_2\text{B}\{\text{CO}_2\text{H}\}$ (15.5 mg, 0.035 mmol) and $\{\text{HCNDipp}\}_2\text{B}\{\text{Br}\}$ (16.5 mg, 0.035 mmol) was dissolved in C_6D_6 (0.5 mL) and NEt_3 then added (5 μL , 0.036 mmol). The mixture was heated at $80\text{ }^{\circ}\text{C}$ for 3 h, showing 25 % conversion by ^1H NMR. After 2 d at $80\text{ }^{\circ}\text{C}$ the reaction slowed down at 70 % conversion, so more NEt_3 (5 μL , 0.036 mmol) was added, and the reaction mixture heated for another 2 d at $80\text{ }^{\circ}\text{C}$, at which point conversion had reached more than 90 %. The solution was transferred into a crystallisation tube (leaving behind crystalline $[\text{Et}_3\text{NH}]\text{Br}$), all volatiles were then removed *in vacuo* and the residue recrystallized from hexane, yielding colourless plates of **3** (18 mg, 0.022 mmol, 63%). The ^1H and ^{11}B NMR spectra matched those measured for samples obtained from the decomposition of **2**.

Reaction of 1 with two equivalents of CO_2 : A solution of **1** (27 mg, 0.030 mmol) in C_6D_6 (0.5 mL) was degassed by the freeze/pump/thaw procedure, and the tube backfilled with CO_2 (ca. 1 atm.) and shaken for 10 min. The ^1H NMR spectrum showed clean formation of a single product (i.e. **2**). The tube was reconnected to the CO_2 ampoule to top up the gas pressure. Monitoring by ^1H NMR showed formation of one major product after 10 days, as the colour changed to pale brown. Volatiles were removed *in vacuo* but attempted crystallisation of the oily residue from hexane or pentane gave only small amount of colourless crystals identified as **5** by X-ray diffraction. The oily product was transferred into an NMR tube with C_6D_6 (0.5 mL) and solid *N,N*-dimethylaminopyridine (DMAP) (6.0 mg, 0.049 mmol) was added. Removal of volatiles and extraction of the residue with warm hexane (the product was sparingly soluble), evaporation of solvent and drying *in vacuo* produced off-white crystals of $\text{Sn}\{\text{O}_2\text{CB}(\text{NDippCH})_2\}_2(\text{DMAP})$, **4**(DMAP), (18 mg, 0.016 mmol, 54 %). X-ray quality crystals of **4**(DMAP)·0.5(C_6H_{14}) were obtained by slow evaporation of solvent from a solution in hexane. Anal. found (calcd. for $\text{C}_{61}\text{H}_{82}\text{B}_2\text{N}_6\text{O}_4\text{Sn}$): C, 66.08 (66.38); H, 7.43 (7.49); N, 7.42 (7.61) %. ^1H NMR (C_6D_6 , 298 K): δ_{H} 7.51 (br m, 2H, *o*-H of DMAP), 7.14–7.21 (m, 12H, *m*- and *p*-H of Ar + $\text{C}_6\text{D}_5\text{H}$), 6.09 (s, 4H, NCH), 5.69 (d, $^3J = 6.2\text{ Hz}$, 2H, *m*-H of DMAP), 3.25 (sept, $^3J = 6.9\text{ Hz}$, 8H, CHMe_2), 2.19 (s, 6H, NMe_2), 1.29 (d, $^3J = 6.9\text{ Hz}$, 24H, CHMe_2), 1.26 (d, $^3J = 6.9\text{ Hz}$, 24H, CHMe_2 + CH_2 of hexane), 0.88 (t, 3H, CH_3 of hexane). ^{13}C -NMR (C_6D_6 , 298 K): δ_{C} 154.4 (*p*-C of DMAP), 147.5 (*o*-CH of DMAP), 146.2 (*o*-C of Ar), 139.3 (*ipso*-C of Ar), 127.4 (*p*-CH of Ar), 123.3 (*m*-CH of Ar), 119.8 (NCH), 106.3 (*m*-CH of DMAP), 38.2 (NMe_2), 31.9 (CH_2 of hexane), 28.7 (CHMe_2), 24.7 (CHMe_2), 24.5 (CHMe_2), 23.0 (CH_2 of hexane), 14.3 (CH_3 of hexane), (BCO_2 was not observed). ^{11}B NMR (C_6D_6 , 298 K): δ_{B} 20.9 (br). ^{119}Sn NMR (C_6D_6): δ_{Sn} -375.3 .

Synthesis of $\text{Sn}\{\text{O}_2\text{CB}(\text{NDippCH})_2\}_2(\text{LiBr})(\text{thf})$ (4**(LiBr)(thf)):** A solution of $(\text{thf})_2\text{Li}\{\text{B}(\text{NDippCH})_2\}$ (45 mg, 0.083 mmol) in C_6D_6 (0.5 mL) was degassed by the freeze/pump/thaw procedure, and the tube was backfilled with CO_2 (to ca. 1 atm.) and gently shaken. A ^1H NMR spectrum measured at this point showed clean formation of a single product. Excess CO_2 was removed from the headspace, the tube was taken into the glovebox and solid SnBr_2 (11.5 mg, 0.042 mmol) was added. The mixture was

sonicated for 10 min until all solid dissolved, forming a clear solution showing a single set of ^1H NMR signals. The mixture was transferred into a two-section crystallization tube and all volatiles removed *in vacuo* at 50 °C. When hexane was added to the oily residue, a white powder (assumed to be LiBr) precipitated. The clear solution was decanted into the second section of the tube, concentrated almost to dryness, and stored at room temperature overnight forming colourless blocks of **4**(LiBr)(thf) (28 mg, 0.025 mmol, 58 %). Anal. found (calcd. for $\text{C}_{58}\text{H}_{80}\text{B}_2\text{BrLiN}_4\text{O}_5\text{Sn}$): C, 61.24 (61.08); H, 7.21 (7.07); N, 4.99 (4.91) %. ^1H NMR (C_6D_6 , 298 K): δ_{H} 7.05–7.13 (m, 12H, *m*- and *p*-H of Ar), 6.08 (s, 4H, NCH), 3.08 (br sept, 8H, CHMe_2), 2.99 (br m, 4H, OCH_2 of thf), 1.30 (br m, 4H, CH_2 of thf), 1.18–1.28 (m, 48H, CHMe_2). $^{13}\text{C}\{^1\text{H}\}$ NMR (C_6D_6 , 298 K): δ_{C} 181.0 (very broad, only observed in HMBC, BCO_2), 145.8 (*o*-C of Ar), 145.7 (*o*-C of Ar), 139.5 (*ipso*-C of Ar), 127.4 (*p*-CH of Ar), 123.2 (*m*-CH of Ar), 120.1 (NCH), 67.6 (OCH_2 of thf), 28.7 (CHMe_2), 25.4 (CH_2 thf), 24.5 (CHMe_2), 24.5 (CHMe_2). $^{11}\text{B}\{^1\text{H}\}$ NMR (C_6D_6 , 298 K): δ_{B} 20.0 (br). ^7Li NMR (C_6D_6 , 298 K): δ_{Li} 0.22 (s). ^{119}Sn NMR (C_6D_6 , 298 K): δ_{Sn} –408.3.

Synthesis of $\text{Sn}\{\text{O}_2\text{CB}(\text{NDippCH})_2\}\{\text{OB}(\text{NDippCH})_2\}(\text{LiBr})(\text{thf})$ (6**):** A solution of $(\text{thf})_2\text{Li}\{\text{B}(\text{NDippCH})_2\}$ (45 mg, 0.083 mmol) in C_6D_6 (0.5 mL) was degassed by the freeze/pump/thaw procedure, and the tube backfilled with CO_2 (to ca. 1 atm.) and gently shaken. ^1H and ^{13}C NMR spectra showed clean formation of the lithium borylcarboxylate. After ca. 17 h, the sample showed more complex spectra, with the ^{13}C NMR spectrum showing a sharp peak at 184 ppm indicative of CO formation. Solid SnBr_2 (11.5 mg, 0.042 mmol) was added and the mixture sonicated for 10 min until a cloudy solution was formed. The ^1H NMR spectrum measured at this point showed that a mixture of products was formed with a major component having two backbone CH peaks at 5.88 and 6.05 ppm (corresponding to BCO_2 and BO moieties). All volatiles were removed *in vacuo* and the residue extracted with hexane (0.5 mL), leaving a white powder (LiBr). Crystallisation from a concentrated hexane solution at room temperature gave **6** as the major product as large colourless blocks, suitable for X-ray diffraction. Additional recrystallisation yielded $\text{Sn}\{\text{O}_2\text{CB}(\text{NDippCH})_2\}\{\text{OB}(\text{NDippCH})_2\}(\text{LiBr})(\text{thf})$ (**6**) (27 mg, 0.024 mmol, 58 %). ^1H NMR (C_6D_6 , 298 K): δ_{H} 7.13–7.21 (2H, m, *p*-CH of Ar + $\text{C}_6\text{D}_5\text{H}$), 7.01–7.11 (10H, m, *m*- and *p*-CH of Ar), 6.05 (2H, s, NCH), 5.88 (2H, s, NCH), 3.34 (2H, septet, $^3J = 6.8$ Hz, CHMe_2), 3.29 (2H, septet, $^3J = 6.8$ Hz, CHMe_2), 3.22 (2H, septet, $^3J = 6.8$ Hz, CHMe_2), 3.06 (2H, septet, $^3J = 6.8$ Hz, CHMe_2), 2.84 (4H, br m, OCH_2 of thf), 1.29–1.32 (16H, br m, CHMe_2 + CH_2 of thf), 1.15–1.27 (36H, m, CHMe_2). $^{13}\text{C}\{^1\text{H}\}$ NMR (C_6D_6 , 298 K): δ_{C} 182.8 (very broad, only observed in HMBC, BCO_2), 147.6 (*o*-C of Ar), 147.5 (*o*-C of Ar), 145.9 (*o*-C of Ar), 145.7 (*o*-C of Ar), 139.8 (*ipso*-C of Ar), 139.4 (*ipso*-C of Ar), 127.6 (*p*-CH of Ar), 127.3 (*p*-CH of Ar), 124.2 (*m*-CH of Ar), 124.1 (*m*-CH of Ar), 123.2 (*m*-CH of Ar), 123.1 (*m*-CH of Ar), 120.4 (NCH), 116.5 (NCH), 67.9 (OCH_2 of thf), 28.8 (CHMe_2), 28.7 (CHMe_2), 28.7 (CHMe_2), 25.2 (CH_2 thf), 25.0 (CHMe_2), 24.9 (CHMe_2), 24.9 (CHMe_2), 24.7 (CHMe_2), 24.5 (CHMe_2), 24.2 (CHMe_2), 23.8 (CHMe_2). $^{11}\text{B}\{^1\text{H}\}$ (C_6D_6 , 298 K): δ_{B} 21.5 (br). ^7Li

NMR (C_6D_6 , 298 K): δ_{Li} –0.30. ^{119}Sn NMR (C_6D_6 , 298 K): δ_{Sn} –287.5.

Alternative synthesis of $\text{Sn}\{\text{O}_2\text{CB}(\text{NDippCH})_2\}_2(\text{DMAP})$ (4**(DMAP)):** Solid potassium hydride (3.0 mg, 0.075 mmol) was added to a solution of $\{(\text{HCNDipp})_2\text{B}\}\text{CO}_2\text{H}$ (23 mg, 0.053 mmol) in C_6D_6 (0.4 mL) and the mixture sonicated for 1 h until no more hydrogen was evolving, and the ^1H NMR spectrum indicated disappearance of the starting compound/formation of $[\text{K}\{\text{O}_2\text{CB}(\text{NDippCH})_2\}]_4$ (**7**). The solution was pipetted into a new NMR tube and the residue (unreacted KH) was washed with C_6D_6 (0.1 mL). Solid SnBr_2 (7.2 mg, 0.026 mmol) was added, but no reaction was observed after sonication for 30 min. Thf (0.1 mL) was then vacuum-transferred into the tube, and sonication continued for another 30 min resulting in a clear solution with a single new set of ^1H NMR signals, but no KBr precipitate. All volatiles were removed *in vacuo*, and the residue was extracted with hexane (0.5 mL), leaving a white powder (assumed to be KBr). Attempted crystallisation from the hexane extract was unsuccessful, and removal of solvent gave a pale brown oil, which showed a similar ^1H NMR spectrum to that of **4** obtained via CO_2 insertion. Addition of DMAP (3.4 mg, 0.028 mmol) resulted in the formation of **4**(DMAP) characterized by a ^1H NMR spectrum identical to that reported above.

Reaction of **1 with N_2O :** A solution of **1** (15 mg, 0.017 mmol) in C_6D_6 (0.5 mL) was degassed by the freeze/pump/thaw procedure, and the tube backfilled with N_2O (ca. 1 atm.) and gently shaken. The colour of the solution changed from yellow-green to dark purple. A ^1H NMR spectrum measured at this point showed formation of a single unsymmetrical product. After storage at room temperature for 12 h the colour changed to light yellow and a complex mixture (including the diazadiene $\text{DippN}=\text{CHCH}=\text{NDipp}$ with backbone CH signal at 8.17 ppm) was formed due to over-oxidation. In order to crystallise the initially formed product, the reaction was carried out in a two-section tube. A solution of **1** (25 mg, 0.028 mmol) in C_6H_6 (0.5 mL) was similarly degassed by the freeze/pump/thaw procedure and treated with N_2O until the colour turned dark purple. The tube was then quickly degassed again by the freeze/pump/thaw to avoid further oxidation, and sealed under vacuum. The solution was concentrated to ca. one quarter volume and stored at room temperature overnight producing deep red-purple crystals of $\text{Sn}\{\text{B}(\text{NDippCH})_2\}\{\text{OB}(\text{NDippCH})_2\}$ (**8**) suitable for X-ray crystallography. ^1H NMR (C_6D_6 , 298 K): δ_{H} 7.15–7.21 (m, 4H, *p*-H of Ar), 7.04–7.07 (m, 8H, *m*-H of Ar), 6.14 (s, 2H, NCH), 6.00 (s, 2H, NCH), 3.33 (septet, $^3J = 6.9$ Hz, 4H, CHMe_2), 3.14 (septet, $^3J = 6.9$ Hz, 4H, CHMe_2), 1.21 (d, $^3J = 6.9$ Hz, 12H, CHMe_2), 1.11 (d, $^3J = 6.9$ Hz, 12H, CHMe_2), 1.06 (d, $^3J = 6.9$ Hz, 12H, CHMe_2), 0.99 (d, $^3J = 6.9$ Hz, 12H, CHMe_2). $^{13}\text{C}\{^1\text{H}\}$ NMR (C_6D_6 , 298 K): δ_{C} 147.3 (*o*-C of Ar), 145.8 (*o*-C of Ar), 139.3 (*ipso*-C of Ar), 138.7 (*ipso*-C of Ar), 127.9 (*p*-CH of Ar), 127.0 (*p*-CH of Ar), 123.7 (*m*-CH of Ar), 123.5 (*m*-CH of Ar), 122.1 (NCH), 116.6 (NCH), 28.8 (CHMe_2), 28.7 (CHMe_2), 24.9 (CHMe_2), 24.7 (CHMe_2), 24.4 (CHMe_2), 24.2 (CHMe_2). $^{11}\text{B}\{^1\text{H}\}$ NMR (C_6D_6 , 298 K): δ_{B} 79.4 (SnB), 24.6 (SnOB).

Conflicts of interest

There are no conflicts to declare.

Acknowledgements

We acknowledge support from the EPSRC (CMcM studentship and EP/K014714/1), the Oxford-SCG Centre of Excellence and the Leverhulme Trust (F/08699/E and RP-2018-246) for funding aspects of this work.

Notes and references

- See, for example, M. Mikkelsen, M. Jørgensen and F. C. Krebs, *Energy Environ. Sci.*, 2010, **3**, 43–81.
- See, for example: (a) K. Huang, C.-L. Sun and Z.-J. Shi, *Chem. Soc. Rev.*, 2011, **40**, 2435–2452; (b) J. Schneider, H. Jia, J. T. Muckerman and E. Fujita, *Chem. Soc. Rev.*, 2012, **41**, 2036–2051; (c) Q. Liu, L. Wu, R. Jackstell and M. Beller, *Nat. Commun.*, 2015, **6**, 5933; (d) L. J. Murphy, K. N. Robertson, R. A. Kemp, H. M. Tuononen and J. A. C. Clyburne, *Chem. Commun.*, 2015, **51**, 3942–3956; (e) A. Tlili, E. Blondiaux, X. Frogneux and T. Cantat, *Green Chem.*, 2015, **17**, 157–168.
- Selected reviews: (a) D. W. Stephan and G. Erker, *Angew. Chem. Int. Ed.*, 2010, **49**, 46–76; (b) L. C. Wilkins and R. L. Melen, “Small Molecule Activation with Frustrated Lewis Pairs” in *Encyclopedia of Inorganic and Bioinorganic Chemistry*, Wiley, Hoboken, NJ, USA, 2011; (c) T. Li, W. Zhang, H. Qin, L. Lu, S. Yan and Z. Zou, *ChemPhotoChem*, 2021, in press (<https://doi.org/10.1002/cptc.202000312>).
- (a) A. Caise, D. Jones, E. L. Kolychev, J. Hicks, J. M. Goicoechea and S. Aldridge, *Chem. Eur. J.*, 2018, **24**, 13624–13635; (b) S. González-Gallardo, V. Jancik, D. Díaz-Gómez, F. Cortés-Guzmán, U. Hernández-Balderas and M. Moya-Cabrera, *Dalton Trans.*, 2019, **48**, 5595–5603; (c) D. Franz, C. Jandl, C. Stark and S. Inoue, *ChemCatChem*, 2019, **11**, 5275–5281; (d) C.-C. Chia, Y.-C. Teo, N. Cham, S. Y.-F. Ho, Z.-H. Ng, H.-M. Toh, N. Mézailles and C.-W. So, *Inorg. Chem.*, 2021, in press (<https://doi.org/10.1021/acs.inorgchem.0c03507>).
- (a) J. A. B. Abdalla, I. M. Riddlestone, R. Tirfoin and S. Aldridge, *Angew. Chem. Int. Ed.*, 2015, **54**, 5098–5102; (b) A. Case, J. Hicks, M. Á. Fuentes, J. M. Goicoechea and S. Aldridge, *Chem. Eur. J.*, 2021, **27**, 2138–2148;
- C. Jenne, M. C. Nierstenhöfer and V. van Lessen, *Chem. Eur. J.*, 2021, **27**, 3288–3291;
- (a) A. Jana, D. Ghoshal, H. W. Roesky, I. Objartel, G. Schwab and D. Stalke, *J. Am. Chem. Soc.*, 2009, **131**, 1288–1293; (b) S. L. Choong, W. D. Woodul, C. Schenk, A. Stasch, A. F. Richards and C. Jones, *Organometallics*, 2011, **30**, 5543–5550; (c) G. Tan, W. Wang, B. Blom and M. Driess, *Dalton Trans.*, 2014, **43**, 6006–6011; (d) T. J. Hadlington, C. E. Kefalidis, L. Maron and C. Jones, *ACS Catal.*, 2017, **7**, 1853–1859.
- (a) M. K. Sharma, C. Wölper, G. Haberhauer and S. Schulz, *Angew. Chem. Int. Ed.*, 2021, **60**, 6784–6790; (b) M. J. Evans, M. D. Anker, C. L. McMullin, N. A. Rajabi and M. P. Coles, *Chem. Commun.*, 2021, **57**, 2673–2676.
- (a) P. Jutzi, D. Eikenberg, A. Möhrke, B. Neumann and H.-G. Stammer, *Organometallics*, 1996, **15**, 753–759; (b) X. Liu, X.-Q. Xiao, Z. Xu, X. Yang, Z. Li, Z. Dong, C. Yan, G. Lai and M. Kira, *Organometallics*, 2014, **33**, 5434–5439; (c) Y. Wang, M. Chen, Y. Xie, P. Wei, H. F. Schaefer III and G. H. Robinson, *J. Am. Chem. Soc.*, 2015, **137**, 8396–8399; (d) F. M. Mück, J. A. Baus, M. Nutz, C. Burschka, J. Poater, F. M. Bickelhaupt and R. Tacke, *Chem. Eur. J.*, 2015, **21**, 16665–16672; (e) D. Wendel, A. Porzelt, F. A. D. Herz, D. Sarkar, C. Jandl, S. Inoue and B. Rieger, *J. Am. Chem. Soc.*, 2017, **139**, 8134–8137; (f) A. Burchert, S. Yao, R. Müller, C. Schattenberg, Y. Xiong, M. Kaupp and M. Driess, *Angew. Chem. Int. Ed.*, 2017, **56**, 1894–1897; (g) A. V. Protchenko, P. Vasko, D. C. H. Do, J. Hicks, M. Á. Fuentes, C. Jones and S. Aldridge, *Angew. Chem. Int. Ed.*, 2019, **58**, 1808–1812; (h) N. Weyer, M. Heinz, J. I. Schweizer, C. Bruhn, M. C. Holthausen and U. Siemeling, *Angew. Chem. Int. Ed.*, 2021, **60**, 2624–2628.
- J. Li, M. Hermann, G. Frenking and C. Jones, *Angew. Chem. Int. Ed.*, 2012, **51**, 8611–8614.
- (a) J. Hicks, A. Heilmann, P. Vasko, J. M. Goicoechea and S. M. Aldridge, *Angew. Chem., Int. Ed.*, 2019, **58**, 17265–17268; (b) D. Anker and M. P. Coles, *Angew. Chem., Int. Ed.*, 2019, **58**, 18429–18433.
- (a) D. Wu, L. Kong, Y. Li, R. Ganguly and R. Kinjo, *Nat. Commun.*, 2015, **6**, 7340; (b) B. Wang, Y. Li, R. Ganguly, H. Hirao and R. Kinjo, *Nat. Commun.*, 2016, **7**, 11871; (c) L. Kong, W. Lu, Y. Li, R. Ganguly and R. Kinjo, *Inorg. Chem.*, 2017, **56**, 5586–5593; (d) K. Ota and R. Kinjo, *Angew. Chem., Int. Ed.*, 2020, **59**, 6572–6575; (e) J. W. Taylor, A. McSkimming, C. F. Guzman and W. H. Harman, *J. Am. Chem. Soc.*, 2017, **139**, 11032–11035; (f) A. Stoy, J. Böhnke, J. O. C. Jiménez-Halla, R. D. Dewhurst, T. Thiess and H. Braunschweig, *Angew. Chem., Int. Ed.*, 2018, **57**, 5947–5951.
- A. Hofmann, M. A. Légaré, L. Wüst and H. Braunschweig, *Angew. Chem. Int. Ed.*, 2019, **58**, 9776–9781.
- C. Weetman, P. Bag, T. Szilvási, C. Jandl and S. Inoue, *Angew. Chem. Int. Ed.*, 2019, **58**, 10961–10965.
- C. Yan, Z. Xu, X.-Q. Xiao, Z. Li, Q. Lu, G. Lai and M. Kira, *Organometallics*, 2016, **35**, 1323–1328.
- (a) C. A. Stewart, D. A. Dickie, Y. Tang and R. A. Kemp, *Inorg. Chim. Acta*, 2011, **376**, 73–79; (b) L. A.-M. Harris, M. P. Coles and J. R. Fulton, *Inorg. Chim. Acta*, 2011, **369**, 97–102.
- (a) A. Jana, H. W. Roesky, C. Schulzke and A. Döring, *Angew. Chem. Int. Ed.*, 2009, **48**, 1106–1109; (b) S. Weiß, M. Wideman, K. Eichele, H. Schubert and L. Wesemann, *Dalton Trans.*, 2021, in press (<https://doi.org/10.1039/D1DT00542A>).
- (a) L. R. Sita, J. R. Babcock and R. Xi, *J. Am. Chem. Soc.*, 1996, **118**, 10912–10913; (b) J. R. Babcock, L. Liable-Sands, A. L. Rheingold and L. R. Sita, *Organometallics*, 1999, **18**, 4437–4441; (c) C. A. Stewart, D. A. Dickie, M. V. Parkes, J. A. Saria and R. A. Kemp, *Inorg. Chem.*, 2010, **49**, 11133–11141; (c) C. A. Stewart, D. A. Dickie, B. Moasser and R. A. Kemp, *Polyhedron*, 2012, **32**, 14–23.
- D. A. Dickie, E. N. Coker and R. A. Kemp, *Inorg. Chem.*, 2011, **50**, 11288–11290.
- (a) A. V. Protchenko, K. H. Birjkumar, D. Dange, A. Schwarz, D. Vidovic, C. Jones, N. Kaltsoyannis, P. Mountford and S. Aldridge, *J. Am. Chem. Soc.*, 2012, **134**, 6500–6503; (b) A. V. Protchenko, J. I. Bates, L. M. A. Saleh, M. P. Blake, A. D. Schwarz, E. L. Kolychev, A. L. Thompson, C. Jones, P. Mountford and S. Aldridge, *J. Am. Chem. Soc.*, 2016, **138**, 4555–4564. See also (c) A. V. Protchenko, M. P. Blake, A. D. Schwarz, C. Jones, P. Mountford and S. Aldridge, *Organometallics*, 2015, **34**, 2126–2129.
- Y. Segawa, Y. Suzuki, M. Yamashita and K. Nozaki, *J. Am. Chem. Soc.*, 2008, **47**, 16069–16079.
- (a) A. V. Protchenko, D. Dange, M. P. Blake, A. D. Schwarz, C. Jones, P. Mountford and S. Aldridge, *J. Am. Chem. Soc.*, 2014, **136**, 10902–10905; (b) S. Jain and K. Vanka, *PCCP*, 2019, **21**, 14821–14831.
- H. Kisu, H. Sakaino, F. Ito, M. Yamashita and K. Nozaki, *J. Am. Chem. Soc.*, 2016, **138**, 3548–3552.
- Y. K. Loh, L. Ying, M. Á. Fuentes, D. C. H. Do and S. Aldridge, *Angew. Chem. Int. Ed.*, 2019, **58**, 4847.
- (a) J. Cosier and A. M. Glazer, *J. Appl. Cryst.*, 1986, **19**, 105–107; (b) CrysAlisPRO, Oxford Diffraction/Agilent Technologies UK Ltd, Yarnton, UK; (c) G. Sheldrick, *Acta Cryst. C*, 2015, **71**, 3–8; (d) G. Sheldrick, *Acta Cryst. A*, 2008, **64**, 112–122; (e) O.

V. Dolomanov, L. J. Bourhis, R. J. Gildea, J. A. K. Howard and H. Puschmann, *J. Appl. Cryst.*, 2009, **42**, 339-341; (f) L. J. Barbour, *J. Appl. Cryst.*, 2020, **53**, 1141-1146.